Magnetic Skyrmions in Condensed Matter Physics*

Sayantika Bhowal,** S. Satpathy, and Pratik Sahu

Department of Physics & Astronomy, University of Missouri, Columbia, MO 65211, USA

Abstract.   Skyrmions were originally introduced in Particle Physics as a possible mechanism to explain the stability of particles. Lately the concept has been applied in Condensed Matter Physics to describe the newly discovered topologically protected magnetic configurations called the magnetic Skyrmions. This elementary review introduces the concept at a level suitable for beginning students of Physics.
Keywords: Skyrmions, Winding number, Spin texture

1.   INTRODUCTION

The basic objects of Classical Mechanics are stable particles, characterized by a non-zero mass, which live for ever. In contrast, at a fundamental level, elementary particles such as electrons and protons are described using quantum field theory, where they are thought of as wave-like excitations of an underlying field. It is however a non-trivial task in field theory to make these wave-like excitations stable; they would generally dissipate similar to the disappearance of the waves in a pond once they have been created. In the year 1962, Skyrme [1] proposed the idea that the particles do not decay because they are topologically protected, in the sense that they have a topological number, which can not be changed by a continuous deformation of the underlying field. In topology, a donut is topologically equivalent to a cup, as they both contain one hole, and one can be continuously deformed to the other. A sphere contains no hole and is topologically different, and thus can not be deformed into a donut by continuous deformation. Sometime later, it was pointed out that topologically protected systems may be relevant in condensed matter physics [2, 3]. Recently, there has been a flurry of theoretical and experimental works [4] showing that topologically protected states can be stabilized in chiral magnets in the form of a swirling spin texture called a "magnetic Skyrmion." The present review aims at introducing the basic concepts of the magnetic Skyrmion to beginning students of Physics.

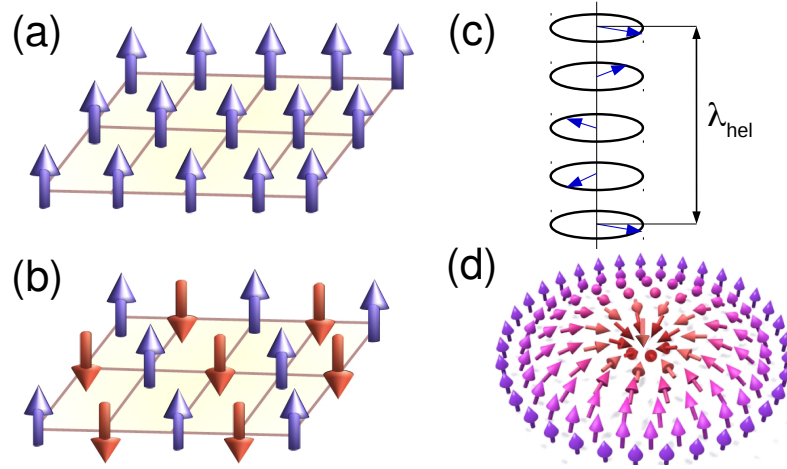## 2.   MAGNETIC INTERACTION IN SOLIDS

In magnetic solids, such as Iron, atoms acquire a magnetic moment due to the spin of the electron, or in some cases due to its orbital motion. Arranged on a periodic lattice structure in the solid, the atomic moments interact with one another, leading to well defined magnetic structures such

---

**bhowals@missouri.edu

Figure 1. Different types of magnetic states in solid. (a) Ferromagnetic state, (b) Anti-ferromagnetic state (c) Helical state, and (d) Skyrmion state. For the ferromagnetic and the anti-ferromagnetic structures, magnetic moments of individual atoms are arranged as shown. In the helical state, ferromagnetic planes are stacked on top of one another, with their magnetic moments turning with the periodicity determined by the helical length λ_{hel}. The Skyrmion state is characterized by a certain Skyrmion number as discussed in the text. (Fig. (d) is reproduced with permission from the authors of Ref. [5].)

as a ferromagnet or an anti-ferromagnet. The simplest Hamiltonian that describes the interaction between the magnetic moments is the Heisenberg Hamiltonian

$$\mathcal{H}_H = J \sum_{ij} \vec{S}_i \cdot \vec{S}_j, \tag{1}$$

where $\vec{S}_i$ is the (spin) magnetic moment at site i and J is the interaction between nearest neighbors. The sign of J determines the relative alignment of the spins, e.g., if $J < 0$, the spins prefer to align parallel to each other (ferromagnet) so that the energy is a minimum. On the other hand, a positive J leads to an antiparallel alignment resulting in an antiferromagnetic structure (See Fig. 1). In solids with strong spin-orbit coupling and broken inversion symmetry, a cross-product or chiral interaction, known as the Dzyaloshinskii-Moriya (DM) interaction exists. Although much smaller in magnitude than the Heisenberg interaction, the DM interaction can lead to fundamentally new Physics. The DM interaction reads

$$\mathcal{H}_{DM} = \sum_{ij} \vec{D}_{ij} \cdot (\vec{S}_i \times \vec{S}_j), \tag{2}$$

where $\vec{D}$ is the strength of the DM interaction. In contrast to the Heisenberg interaction which only favors parallel or antiparallel alignment of the spins, the DM interaction favors a canted spin
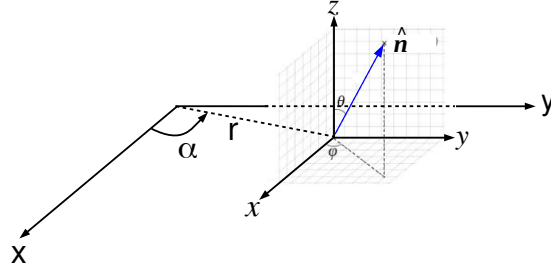
Figure 2. Polar coordinates to describe the spin texture in the continuum model of the Skyrmion state. The direction of the magnetization vector $\vec{n}(\vec{r})$ depends on its location $\vec{r}$ on the 2D plane, described by the polar coordinates (r, α), but $\vec{n}(r, \alpha)$ can point anywhere in 3D, described by the spherical coordinates θ and ϕ at each point $\vec{r}$. For the skrmion state, the polar angle $\theta(r)$ and the azimuthal angle $\phi(\alpha)$ are functions of only r and α, respectively. An electron moving in the spin texture $\vec{n}(\vec{r})$ experiences a topological electric amd magnetic field, caused by the fact that the electron spin must follow the local spin directions as it moves in the 2D space.

alignment (energy becomes minimum if the two spins are perpendicular to each other and lie on a plane normal to $\vec{D}$, as can be immediately seen from Eq. 2).

The presence of both the Heisenberg and the DM interactions leads to a helical spin state, and the DM interaction under certain conditions can lead to the Skyrmion state as well, which we will discuss shortly. In the simplest helical state, ferromagnetic planes of spins turn along the direction normal to the planes, with a helicity angle ϑ and the helical period $\lambda^{\text{hel}} = 2\pi/\vartheta$ (Fig. 1 c). The helicity angle is determined by the minimization of the net energy, coming directly from the expressions for the Heisenberg and the DM interactions,

$$E(\vartheta) = JS^2 \cos \vartheta + DS^2 \sin \vartheta, \tag{3}$$

which leads to $\vartheta = \tan^{-1}(D/J)$. The helical period ($\lambda^{\text{hel}}$) in some representative materials are listed in Table 1, which is indicative of the strength of the DM interaction.

3. THE SKYRMION STATE

The Skyrmion state is a complex magnetic state, the formation of which is mediated by one of several mechanisms [6–9], viz., (i) The DM interaction together with a magnetic field, (ii) Magnetic dipolar interaction, (iii) Frustrated exchange interaction, (iv) Four-spin interactions, and (v) Rashba spin-orbit coupling in the presence of itinerant electrons (polaronic Skyrmion).

In addition, the Skyrmion state is defined such that $\theta(r)$ changes from $\theta = \pi$ at the center

Table 1. Néel temperatures (T_N) and helical periods (λ^{hel}) in some of the magnetic materials with broken inversion symmetry.

Materials	T_N (K)	λ^{hel} (nm)
MnSi (Bulk)	30	18
MnSi (Thin film)	45	8.5
MnGe (T = 20 K)	170	3
$Mn_{0.5}Fe_{0.5}Ge$	185	14.5

to $\theta = 0$ at the boundary of the Skyrmion ($r = \lambda$) or vice versa. Single-valuedness of the spin orientation demands that the azimuthal angle is of the form
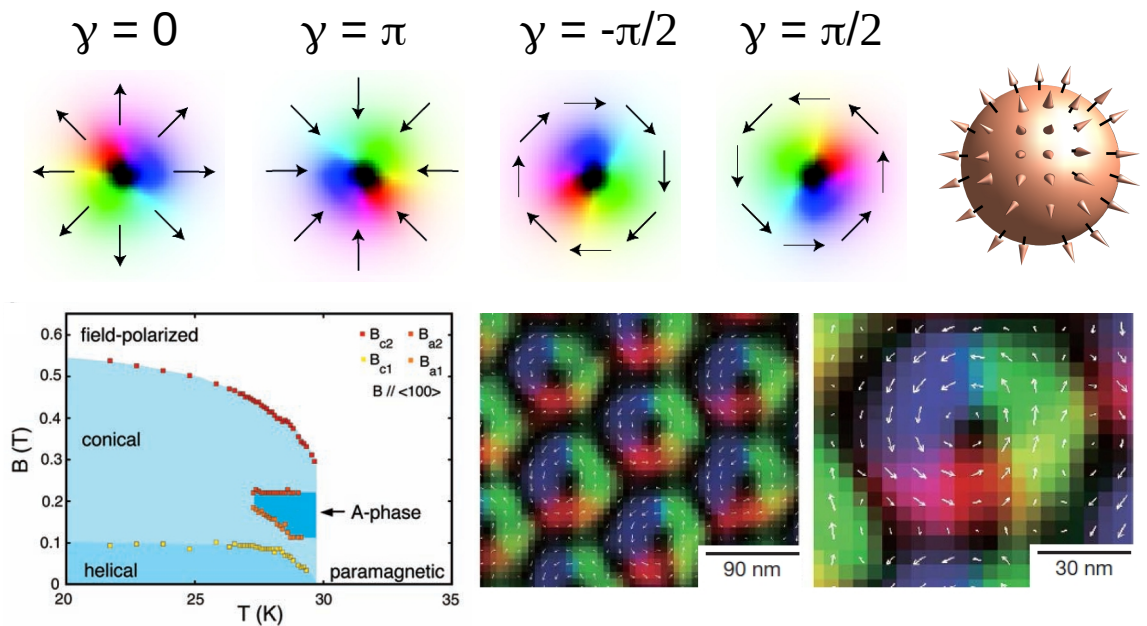
$$\phi(\alpha) = m\alpha + \gamma, \qquad \text{(winding number } m \text{ and helicity parameter } \gamma \text{ defined)} \quad (4)$$

A magnetic Skyrmion is a swirling magnetic structure of spins as illustrated in Fig 1. It is usually a two-dimensional (2D) object, existing at interfaces between two materials or in magnetic thin films. The topological properties depend on the geometry of the structure. The two key characteristic geometrical quantities are the vorticity and the helicity of the structure, which are a characteristic of how the spin orientation $\vec{n}(\vec{r})$ changes over space. Note that for the lattice, the position $\vec{r}$ takes discrete values, while in continuum models it is a continuous variable. The spin orientation at each point $\vec{r} \equiv (r, \alpha)$ on the 2D plane is described in the spherical coordinates by specifying the polar and azimuthal angles, $\theta(\vec{r})$ and $\phi(\vec{r})$, respectively, as indicated in Fig. 2. For the Skyrmion state, $\theta(\vec{r})$ is a function of the radial distance r only and $\phi(\vec{r})$ is a function of the polar angle α only, so that in the cartesian coordinates, the local magnetization vector is

$$\vec{n}(\vec{r}) = (\sin\theta(r)\cos\phi(\alpha), \sin\theta(r)\sin\phi(\alpha), \cos\theta(r)). \tag{5}$$

where $\phi(\alpha)$ is given in Eqn.(4) with m is a non-zero integer called the winding number. Skyrmions and anti-Skyrmions are defined as those for which the winding number is positive or negative, respectively. The helicity parameter γ takes specific values for helical states. If $\gamma = \pm\pi/2$, then the helicity $h = \pm 1$ (the two signs indicate left or right handedness), while for $\gamma = 0$ or π, we have a radial spin structure. The Skyrmion spin texture for the winding number $m = 1$ and for different helicity parameters $\gamma = 0, \pi, \pm\pi/2$ are shown in Fig. 3 for illustration.

Physically speaking, a 2D magnetic Skyrmion can be thought of as a topological object which is formed by a stereographic projection from a spherical "hedgehog" of spins as shown in Fig. 3, where the down spin at the south-pole is mapped onto the center of the 2D disk, while the up spin at the north-pole is mapped onto the edge circle of the disk, far off from the centre. The Skyrmion number N_{sk} denotes the number of times $\vec{n}(\vec{r})$ wraps around the unit sphere. As shown in Section 5, the Skyrmion number simply equals the winding number m apart from a sign. Note that for trivial magnetic structures, e.g., ferro and antiferromagnetic order, $N_{sk} = 0$, while for the example shown in Fig. 3, the Skyrmion number is one.

Figure 3. *Top panel:* Several Skyrmion spin structures corresponding to the winding number $m = 1$ and helicity parameter $\gamma = 0, \pi, \pm\pi/2$. The in-plane components of the spins are indicated by arrows, while the color map denotes the out of-plane component of the spin, where the black and white colors represent the down and up spin state, respectively. *Top panel right:* The spherical "hedgehog" of spins, the stereographic projection of which leads to the 2D magnetic Skyrmion as discussed in the text. The figure corresponds to the winding number $m = 1$. *Bottom left:* The phase diagram of MnSi in the parameter space of temperature (T) and magnetic field (B), showing the stabilization of the Skyrmion phase (the so called "A-phase") with small external magnetic field. *Bottom middle:* The real space configuration of the Skyrmion crystal in $Fe_{0.5}Co_{0.5}Si$ subjected to a weak magnetic field. *Bottom right:* The magnified view of this Skyrmion spin texture. The direction of the spin at each point is described by the color map: black color denotes ↑ or ↓ spin and the white arrows denote the in-plane component. Figure reproduced with permission from: top panel, Ref. [4] © 2013 Springer Nature; bottom left, Ref. [10] © 2009 AAAS; bottom middel and right, Ref. [11] © 2010 Springer Nature.

Experimental observation – Skyrmions were first observed in the year 2009 in MnSi using neutron scattering [10], when the well-known A-phase of MnSi was identified as the Skyrmion phase (Fig. 3). As shown in the figure, the Skyrmion lattice was stabilized at the boundary between the paramagnetic phase and a long-range helimagnetic phase, under the application of a small external magnetic field. The DM interaction induced by the symmetry-breaking distortions in the B20

phase [12] plays a crucial role in stabilizing the Skyrmion state in MnSi. Since then, other experiments have confirmed the existence of the Skyrmion state in a large number of chiral magnets, such as MnGe, $Fe_{1-x}Co_xSi$, etc [13]. More recently, experiments have shown the emergence of the Skyrmion state in oxide heterostructures [14, 15], when subjected to an external electric field. Such magnetic Skyrmion states are shown to be tunable by the external electric field, which controls the DM interaction at the interface [15].

In solids, the Skyrmions often form a periodic lattice (the Skyrmion crystal), rather than occurring as a single isolated Skyrmion. The Skyrmion crystal has a lattice structure, different from the atomic lattice of the host with a lattice spacing $\sim 50 - 100$ times larger than that of the underlying atomic lattice. The Skyrmion crystal phase can be detected by neutron scattering and usually small-angle neutron scattering (SANS) is employed for this purpose. An alternative technique is the resonant X-ray scattering. While these are momentum-space techniques, other methods such as the scanning probe microscopy are suitable for the direct real-space detection of the Skyrmion crystal or the isolated Skyrmions at the nanometre scale.

4. SKYRMION FORMATION: THE DZYALOSHINSKII-MORIYA MECHANISM

In this Section, we describe the formation of the Skyrmion state due to the DM interaction, which is a key mechanism. For the Skyrmion state to form, its energy must be lower than other competing magnetic states. For this to happen, certain types of magnetic interactions need to be present. According to the scaling argument of Derrick [16], formation of the Skyrmion state requires an odd power of the spatial gradient of $\vec{n}(\vec{r})$ (note that $\vec{n}$ is simply the direction of the spin $\vec{S}$) in the energy expression. In these models, the magnitude of $\vec{S}$ remains the same everywhere in space, but their orientation can change depending on the interaction.

The simplest model that can host the Skyrmion state has the DM interaction, which contains the gradient $\vec{\nabla}\vec{n}$ to the first power. Using familiar notations, the Hamiltonian reads

$$\mathcal{H} = J\sum_{ij}\vec{S}_i \cdot \vec{S}_j + \sum_{ij}\vec{D}_{ij} \cdot (\vec{S}_i \times \vec{S}_j) - A_s\sum_i(S_i^z)^2 - B\sum_i S_i^z, \tag{6}$$

where we have considered a spin model for a 2D system, where J is the FM Heisenberg exchange interaction, D is the DM interaction, A_s is the single-ion anisotropy, and B is an external magnetic field. It can be immediately seen by inspection of the Hamiltonian in the continuum limit, Eq. (7), that the DM interaction contains the only odd-power gradient term and therefore without it, a Skyrmion can not exist.

For the purpose of illustration, we take the DM interaction of the form[17] $\vec{D}_{ij} = D\ \hat{r}_{ij} \times \hat{z}$, which may arise from the Rashba SOC at a 2D interface [17], and write the Hamiltonian (6) in the continuum limit. The result is

$$E = \int d^2r\Big[\frac{J}{2}\sum_{\mu=x,y,z}(\vec{\nabla}n^\mu)^2 + D(n^z\partial_x n^x - n^x\partial_x n^z - n^y\partial_y n^z + n^z\partial_y n^y)$$
$$-A_s(n^z)^2 - Bn^z\Big], \tag{7}$$
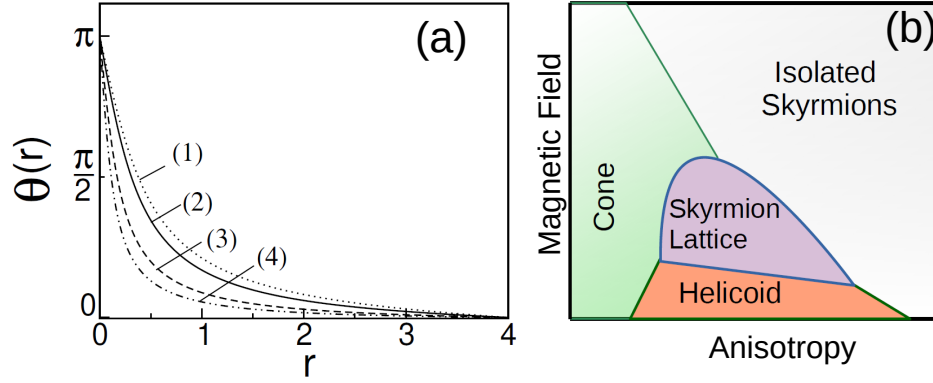
Figure 4. (a) Skyrmion solution of the second order differential equation (8) for the parameters (α, β, γ): (1) (0.2, 0.0, 0.1), (2) (0.2, 0.1, 0.0), (3) (0.2, 0.1, 0.1), and (4) (0.2, 0.1, 0.2). Here, the value of r, at which $\theta(r) = 0$, determines the Skyrmion size λ, which is a function of the parameters α, β, and γ, and has the typical value $\lambda \sim 100 - 1000$ Å in real materials. (b) The schematic phase diagram, adopted from Ref. [18], showing the equilibrium states for the model spin Hamiltonian (6) of a cubic helimagnet as a function of applied magnetic field (B) and uniaxial anisotropy (A_s). The scale of the magnetic field here is $B \sim 0.1 - 1$ Tesla, which is the typical value for which skyrmions have been observed in real materials (See Fig. 3).

where $\vec{\nabla} \equiv \hat{x}\partial_x + \hat{y}\partial_y$. Note that if $D = 0$, then a uniform ferromagnetic state ($\vec{n}$ along $\hat{z}$) has the lowest energy, since any spatial deviation of the spin direction from $\hat{z}$ increases the total energy, and therefore any other state including the Skyrmion state would have a higher energy. This is a simple consequence of Derrick's stability criterion, since if $D = 0$ in the energy expression (7), then no odd power of $\vec{\nabla}\vec{n}$ is present anymore. Substituting the spin texture for the Skyrmion, Eq. (5), in the energy expression (7) and after some straightforward algebra, we get the expression for the energy of the Skyrmion state

$$E = 2\pi \int r\, dr \left[\frac{J}{2}(\dot{\theta}_r^2 + \sin^2\theta/r^2) + D(\dot{\theta}_r + \sin 2\theta/2r) - A_s \cos^2\theta - B\cos\theta \right], \quad (8)$$

where we have considered a Skyrmion with unit vorticity ($m = 1$).

The problem now boils down to the minimization of the energy, which can be done using the standard methods of the calculus of variations, which leads to the Euler equation

$$\frac{d}{dr}\left(\frac{\partial F}{\partial \dot{\theta}_r}\right) = \frac{\partial F}{\partial \theta}, \quad (9)$$

where $F \equiv F(\theta, \dot{\theta}_r, r)$ is the integrand in (8). Taking the derivatives, we immediately get a second-order differential equation

$$\ddot{\theta}_r + \dot{\theta}_r/r + \alpha \sin^2 \theta/r - \beta \sin 2\theta - \sin 2\theta/r^2 - \gamma \sin \theta = 0, \qquad (10)$$

where we have defined the scaled parameters $\alpha = 2D/J$, $\beta = A_s/J$, and $\gamma = B/J$. These are the scaled DM, anisotropy, and the magnetic field parameters, respectively.

The solution of the differential equation is obtained with the finite difference method with the boundary conditions: $\theta(r = 0) = \pi$ and $\theta(r \to \infty) = 0$, with various values of the parameters α, β and γ. The results are shown in Fig. 4 (a), which indicate the formation of an isolated Skyrmion state. Note that the magnetic field (parameter γ) aids in the formation of the Skyrmion state, and as the strength of the field is increased, the size of the Skyrmion becomes smaller and smaller.

So far we have discussed the role of the DM interaction in the formation of an isolated Skyrmion state in 2D. In reality, other spin textures such as the cone phase and the helicoid structure can also be stabilized. The stabilizations of these different magnetic states as a function of external magnetic field and anisotropy are discussed in Ref. [18] in the context of cubic helimagnets. A schematic of this phase diagram is shown in Fig. 4 (b).

5. DYNAMICS OF ELECTRONS IN THE PRESENCE OF A SKYRMION: THE TOPO-LOGICAL MAGNETIC FIELD

In this Section, we discuss the forces acting on an itinerant electron as it moves through the Skyrmion state, with the local space fixed magnetic moments defined by $\vec{n}(\vec{r})$. The topological electromagnetic fields are effective fields that the electron sees on account of its motion in the network of the localized moments. We assume a strong Hund's coupling, which means that the only possible spin state of the electron is the one parallel to the magnetization vector of the local spin. Thus as the electron moves about in space, its spin must conform to the local magnetization direction. An effective electromagnetic field arises, even though no external electric or magnetic field has been applied. These are the so called "emergent" or "topological" fields that the electron experiences because the local magnetization vector changes from point to point.

Let us consider an electron moving in a spatially varying spin texture of the Skyrmion state, with the local magnetization vector $\vec{n}(\vec{r})$ described by (θ, ϕ) in the spherical coordinates (see Fig. 2). We take the large Hund's coupling limit ($J_H \to \infty$, typically a few eV in the solid), so that the electron spin is everywhere parallel to the local moment as it moves about in the presence of the Skyrmion. Thus the spin wave function of the electron can be written as

$$|\chi(\vec{r})\rangle = \begin{bmatrix} \cos \frac{\theta(r)}{2} e^{-i\phi(\alpha)} \\ \sin \frac{\theta(r)}{2} \end{bmatrix} \qquad (11)$$

in the global spin up ($\uparrow$) and down ($\downarrow$) basis set. As a result, the spin of the electron rotates spatially as if it experiences an effective magnetic field $\vec{B}(\vec{r})$ and precesses about this magnetic field. This
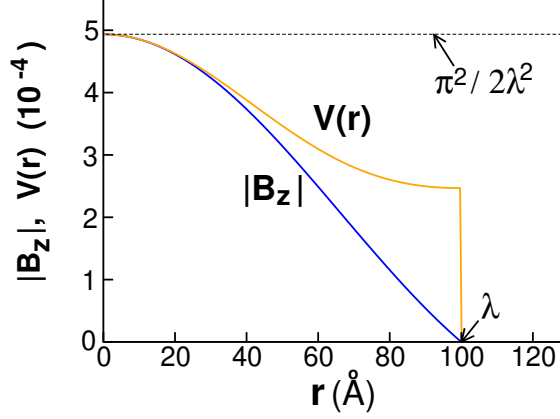
Figure 5. Spatial variations of the topological magnetic field (17) and the scalar potential $V(r)$ (18) for the Skyrmion profile, Eq. (16). The radius of the Skyrmion λ is taken to be 100 Å. For this figure, we have taken $\hbar = c = e = 1$.

physical picture is easy to follow from the kinetic energy of the conduction electron moving in a Skyrmion spin texture $\vec{n}(\vec{r})$,

$$E_{kin} = \langle \Psi | (-\hbar^2 \nabla^2 / 2m) | \Psi \rangle, \tag{12}$$

where the wave function is a direct product of a spatial part and a spin part, viz.,

$$|\Psi\rangle = \psi(\vec{r})\chi(\vec{r}\sigma). \tag{13}$$

Writing $\nabla^2 = \partial_r^2 + \frac{1}{r}\partial_r + \frac{1}{r^2}\partial_\alpha^2$ and $|\Psi\rangle = \psi(r, \alpha)(\cos\frac{\theta(r)}{2}e^{-i\phi(\alpha)}|\uparrow\rangle + \sin\frac{\theta(r)}{2}|\downarrow\rangle)$, and taking into account the symmetry of the Skyrmion i. e., $\theta \equiv \theta(r)$ and $\phi \equiv \phi(\alpha)$, after some algebra we get the kinetic energy of the electron

$$E_{kin} = \frac{-\hbar^2}{2m}\int d^2r\left[\psi^\star\nabla^2\psi - |\psi|^2\left(\frac{\dot{\theta}_r^2}{2} + \frac{\dot{\phi}_\alpha^2\cos^2\theta/2}{r^2}\right) - i\frac{2\dot{\phi}_\alpha\cos^2\theta/2}{r^2}\psi^\star\dot{\psi}_\alpha\right]$$
$$= \frac{1}{2m}\int d^2r\,\psi^\star\left[(\vec{p} - e\vec{A}/c)^2 + V\right]\psi, \tag{14}$$

where $\vec{p} \equiv -i\hbar\vec{\nabla}$, $e < 0$ is the charge of the electron, and the derivatives are indicated by the subscripts, e.g., $\dot{\psi}_\alpha \equiv \partial\psi/\partial\alpha$. Also, here, $V = 4^{-1}\hbar^2\left(r^{-2}\dot{\phi}_\alpha^2\sin^2\theta + \dot{\theta}_r^2\right)$, $\vec{A} = \frac{\Phi_0}{2\pi r}(\dot{\phi}_\alpha\cos^2\theta/2)(\hat{r}\times\hat{z})$ with V and $\vec{A}$ being the scalar and the vector potentials respectively, and $\Phi_0 = hc/e$ is the flux quantum in cgs units. The scalar potential corresponds to a radially outwards force, while the vector

potential $\vec{A}$ leads to the topological magnetic field

$$\vec{B}(\vec{r}) = \vec{\nabla} \times \vec{A} = \hat{z}(\partial_x A_y - \partial_y A_x) = \hat{z}\frac{\Phi_0}{2\pi}\frac{\dot{\theta}_r\dot{\phi}_\alpha \sin\theta}{2r} \tag{15}$$

$$= \frac{\Phi_0}{4\pi}\vec{n}\cdot\left(\partial_x\vec{n}\times\partial_y\vec{n}\right)\hat{z}. \quad \text{(topological magnetic field)}$$

We pause here to consider the special case where the magnetization vector $\vec{n}$ points along $\hat{z}$ everywhere ($\theta = \phi = 0$), for example, for the case of the ferromagnetic state. Then clearly both the scalar and vector potentials are zero from the above expressions and the electron moves as a free particle. In the Skyrmion state, however, the electron experiences a spatially varying topological magnetic field. Let us assume the Skyrmion profile

$$\theta(r) = \pi(1 - r/\lambda), \ r \le \lambda$$
$$= 0, \ r > \lambda$$
$$\text{and} \quad \phi(\alpha) = \alpha, \tag{16}$$

where λ denotes the Skyrmion radius. Using these functional forms of $\theta(r)$ and $\phi(\alpha)$, it is easily seen that the topological magnetic field is along $\hat{z}$ with the magnitude

$$B_z = -\frac{\Phi_0}{4\lambda r}\sin(\pi r/\lambda), \ \text{if} \ r \le \lambda$$
$$= 0, \ \text{if} \ r > \lambda, \tag{17}$$

and

$$V(r) = 4^{-1}\hbar^2\left[\frac{\sin^2(\pi r/\lambda)}{r^2} + \frac{\pi^2}{\lambda^2}\right], \ \text{if} \ r \le \lambda$$
$$= 0, \ \text{if} \ r > \lambda. \tag{18}$$

The spatial variation of these quantities are shown in Fig. 5. As can be seen from these plots, at the centre of the Skyrmion ($r \to 0$) $|B_z| = V(r) = \pi^2/2\lambda^2$. For typical Skyrmion radius $\lambda = 100$ Å, this leads to a large topological magnetic field ($\sim 10^2$ Tesla), which thus provides a unique platform to study the high magnetic field response of electrons [19].

Tight-Binding description – In the above analysis, we obtained the topological magnetic field from a continuum description, while in the solids, the Skyrmions exist of course on crystal lattices. A different way of obtaining the topological magnetic field is to consider the phase accumulated by the traveling electron in the lattice. As the electron travels, its spin must follow the fixed local magnetization direction $\vec{n}(\vec{r})$ adiabatically, as we already discussed. The hopping matrix element between two lattice sites a and b, in the tight-binding theory becomes

$$t_{ab} = \langle\Psi_a|H|\Psi_b\rangle = \langle\psi_a|H|\psi_b\rangle \times \langle\chi_a|\chi_b\rangle = te^{i\eta}, \tag{19}$$
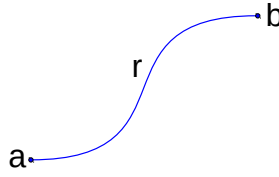
Figure 6. In the presence of a magnetic field, the amplitude to go from point a to point b acquires an extra phase factor $\left[\exp \left(\frac{ie}{\hbar c} \int_a^b \vec{A} \cdot d\vec{r} \right) \right]$, where $\vec{A}$ is the magnetic vector potential, as discussed in the Feynman Lecture Notes [20]. This modifies the hopping amplitude in the tight-binding theory as indicated in Eq. 20.

where $t = \langle \psi_a | H | \psi_b \rangle$ is the electron hopping without the spin texture and in the last equality, we have assumed a slowly varying spin texture (i. e., change in θ and ϕ between nearest neighbors in the lattice is assumed to be small). As is well known from the seminal book by Feynman [20], when an electron moves in a magnetic field, it acquires a phase factor (see Fig. 6), viz.,

$$t_{A \neq 0} = t_{A=0} \times \exp \left(\frac{ie}{\hbar c} \int_a^b \vec{A} \cdot d\vec{r} \right). \tag{20}$$

Comparing Eqs. (19) and (20), it is clear that even though no external magnetic field is present, the adiabatic motion of the electron in the spin texture is equivalent to a magnetic field, the "topological" magnetic field. Expressing the phase factor in Eq. (19) in terms of the Skyrmion texture $\theta(\vec{r})$ and $\phi(\vec{r})$ and after some straightforward algebra, one again gets the expression Eq. (15) for the topological magnetic field $\vec{B}(\vec{r})$.

Magnetic flux through the Skyrmion – It is easy to show that the flux through the Skyrmion due to the topological magnetic field is an integer multiple (the Skyrmion number N_{sk}) of the flux quantum Φ_0. Computing the flux through the 2D surface containing the Skyrmion with the magnetic field Eq. (15), we have

$$\Phi = \int_S \vec{B} \cdot d\vec{S} = \frac{\Phi_0}{4\pi} \int \left[\vec{n} \cdot \left(\partial_x \vec{n} \times \partial_y \vec{n} \right) \right] dS = \Phi_0 N_{sk}, \tag{21}$$

where the Skyrmion number N_{sk} characterizes the swirling structure of the Skyrmion. The fact that the Skyrmion number is an integer is a simple consequence of the boundary conditions imposed on $\vec{n}(\vec{r})$ to define the Skyrmion state. Using the Skyrmion spin texture Eq. (5), we can immediately see that the Skyrmion number is simply the winding number m times a sign $\eta = \pm 1$,

$$N_{sk} = \frac{1}{4\pi} \int_0^\infty dr \sin \theta(r) \dot{\theta}_r \times \int_0^{2\pi} d\alpha \, \dot{\phi}_\alpha = \eta m. \tag{22}$$

The quantity $\eta = \frac{1}{2} \cos \theta(r)|_{r=0}^{r=\infty} = \pm 1$ is related to the magnetization direction at the origin, i. e., if the spins point up at the origin $(r = 0)$ and down at $r \to \infty$, then $\eta = +1$, and it is -1 in the opposite case.

6. SKYRMIONIC POLARON

In this Section, we discuss the idea whether an electron can nucleate a Skyrmion state. The term "Skyrmionic polaron" has been recently coined [9] to describe such a system, which is analogous to the standard polaron state, which is a combination of an electron and the distorted lattice, which together form a localized state due to the electron-phonon interaction.

Interfaces are of interest because they are fertile grounds for the experimental observation of the Skyrmions. It has been recently suggested that the Skyrmionic polaron may exist at the interface between two solids, aided by the so called Rashba spin-orbit coupling [21]. The idea is that due to the broken mirror symmetry, an electric field perpendicular to the interface plane can exist, and if a large spin-orbit coupling is present, they both together lead to the momentum-dependent spin splitting of the electron states at a surface or interface, known as Rashba effect [21].

Rashba spin-orbit interaction – The Rashba interaction is a relativistic effect, originating from the coupling between the spin and the orbital degrees of freedom, when an electric field is present along a certain direction. This happens in solids when the mirror symmetry is broken, e.g., at the surface or at the interface between two materials. The Rashba interaction is described by the Hamiltonian

$$\mathcal{H}_R = \alpha_R(\sigma_x k_y - \sigma_y k_x), \tag{23}$$

where $\vec{k}$ is the electron momentum, $\vec{\sigma} = (\sigma_x, \sigma_y, \sigma_z)$ are the Pauli matrices, and α_R is the strength of the Rashba interaction. Diagonalization of (23) leads to the additional linear splitting term on top of the quadratic band structure energy, with the result $\varepsilon_k = (\hbar^2 k^2 / 2m) \pm \alpha_R k$.

The microscopic origin of the Rashba interaction is similar to the relativistic effect that leads to the well-known $\lambda \vec{L} \cdot \vec{S}$ term in the atoms. Consider an electron moving in an electric field $E\hat{z}$, relevant for the Rashba problem. Due to the relativistic effect, in its rest frame, the electron sees the electric field as a magnetic field $\vec{B} = -(\vec{v} \times \vec{E})/c^2$, which couples with the spin magnetic moment. The interaction energy is given by $\mathcal{H}_R = -\vec{M} \cdot \vec{B} = (g\mu_B \vec{\sigma}/2) \cdot (\vec{v} \times \vec{E})/c^2$. Writing $\vec{v} = \hbar \vec{k}/m$ and rearranging the terms, one immediately finds the Rashba Hamiltonian (23), with the Rashba coefficient α_R is expressed in terms of the various fundamental quantities. In addition, one can easily show that if instead of the uniform field along a fixed direction, the nuclear electric field along the radial direction is used, we would obtain the well-known $\lambda \vec{L} \cdot \vec{S}$ term in atomic physics.

The Rashba interaction leads to many interesting phenomena in condensed matter physics, but relevant for the present case is the fact that it produces a Dzyaloshiski-Moriya interaction $\vec{D} \cdot (\vec{S}_i \times \vec{S}_j)$ between two local spins [17], which facilitates the formation of a Skyrmion state by supporting a non-collinear alignment of the spins. So, the question that naturally arises is whether a single electron with the Rashba interaction in a 2D system can nucleate a Skyrmion state for the local spins.

Formation of the Skyrmionic polaron– Consider the following continuum model for a single electron moving in the Skyrmionic spin texture $\vec{n}(\vec{r})$ in the presence of the Rashba interaction. The

Hamiltonian is

$$\mathcal{H} = \frac{\hbar^2 k^2}{2m} - J\vec{n} \cdot \vec{\sigma} + (\sigma_x k_y - \sigma_y k_x) - b_z \int n_z(\vec{r}) \, d^2 r, \tag{24}$$

where we have added a magnetic field b_z normal to the plane for generality because in certain situations, the Skyrmion state is stabilized by a magnetic field, and the exchange coupling J between the local spin texture and the electron spin will be taken as ∞. The large $J \to \infty$ condition effectively renders this to a spinless problem as the electron spin is always parallel to the spin texture $\vec{n}(\vec{r})$ everywhere as the electron moves around. Switching to the spin basis to be along the local moments (Eq. 11), and modeling the Skyrmion texture $\vec{n}(\vec{r})$ again by the form: $\theta(r) = \pi(1 - r/\lambda)$, $r \leq \lambda$, and 0 otherwise, and $\phi(\alpha) = \alpha$, the spinless electron experiences the magnetic field as well as a static potential given by Eqs. (17) and (18), respectively.

We can then proceed to obtain the ground state configuration of the Skyrmion by minimizing the total energy of the Hamiltonian (24) from the variational method, treating the Skyrmion radius λ as the single variational parameter. The average topological magnetic field has the value $\bar{B} = \Phi_0/(\pi\lambda^2)$ and the corresponding magnetic length $l = \lambda/\sqrt{2}$. The quantized electron states of the electron moving in a magnetic field are the Landau levels, with the lowest energy being $\hbar\omega_c/2 = \hbar^2/(m\lambda^2)$, ω_c being the cyclotron radius. The potential energy may be approximated as $\langle V(r) \rangle = V(l)$, where we simply evaluate the expression (18) for $V(r)$ at $r = l$.

The third term in the Hamiltonian (24) is the Rashba term. We evaluate the Rashba energy for the symmetric wave function $\psi(r)$, where there is no angular dependence α, with the result

$$H_R = \langle \psi(r) \uparrow |\alpha_R(k_x \sigma_y - k_y \sigma_x)|\psi(r) \uparrow \rangle = \frac{\alpha_R}{2} \int |\psi|^2 \times (\dot{\theta}_r - \frac{\dot{\phi}_\alpha}{r} \sin\theta) \, d^2 r, \tag{25}$$

where $\uparrow$ denotes the spin aligned along the local moment and $\vec{k} \equiv -i\vec{\nabla}$. Evaluating this integral and putting together all energy terms, we finally arrive at the result

$$E(\lambda) = \frac{\hbar^2 a}{2m\lambda^2} + \pi b_z \lambda^2 (1 - \frac{4}{\pi^2}) - \frac{\alpha_R b}{\lambda}, \tag{26}$$

where $a = \pi^2/4 + 2 + 2^{-1}\sin^2(\pi/\sqrt{2})$ and $b = \pi/2 + 2^{-1/2}\sin(\pi/\sqrt{2})$ are numerical constants, and the three terms are respectively the kinetic energy, the external magnetic field energy, and the Rashba energy. Minimizing the energy $dE(\lambda)/d\lambda = 0$ with no external magnetic field ($b_z = 0$), we obtain the Skyrmion radius and the corresponding ground state energy. The result is

$$\lambda_0 \approx \frac{2\hbar^2}{m\alpha_R}, \quad \text{and} \quad E_0 \approx -\frac{3m\alpha_R^2}{4\hbar^2}. \tag{27}$$

Clearly, without any Rashba interaction ($\alpha_R = 0$), the Skyrmion radius λ_0 is infinity, indicating that there is no Skyrmion state, while the presence of the Rashba term favors the formation of the Skyrmion state with the binding energy E_0. The result is that the electron nucleates the Skyrmion state and in turn becomes bound inside it, forming thereby the "Skyrmionic polaron." From Eq. (26), it can be seen that an external magnetic field further aids in the formation of the Skyrmionic polaron, making its radius smaller and the binding energy larger.

7. APPLICATIONS AND FUTURE PERSPECTIVE

The topic of the magnetic Skyrmions has been rapidly developing over the past few years, both from the viewpoint of fundamental physics as well as the prospect for technological applications [22]. The Skyrmion spin texture is topologically stable with small thermal and quantum fluctuations, which makes it suitable for applications in memory devices. The unusual electron dynamics and transport properties such as the Topological Hall effect (THE) [4, 13, 23] could have important application in spintronics devices. While the first discovery of the Skyrmions occurred in bulk materials with chiral magnetic interactions, the realization that they can also be stabilized at the interfaces of magnetic multilayers [24] has opened up additional potential opportunities, including novel pathways for Skyrmion generation and manipulation.

A promising application involves the so called Topological Hall effect (THE). In the well-known classical Hall effect, discovered by Edwin H. Hall in 1879, when a current carrying conductor is placed in a magnetic field, the charges experience a Lorentz force in a direction perpendicular to both the magnetic field and the current flow. In contrast to this, in the Topological Hall effect, it is the topological magnetic field of a non-collinear spin system such as the Skyrmion gives rise to the Lorentz force on the conduction electron, resulting in a different type of Hall effect. At the same time, the motion of the Skyrmion itself leads to a temporal variation of the topological magnetic field. This, in turn, induces an electromotive force or potential according to the Faraday's law. This topological electric field gives an additional contribution to the Hall effect. This has been observed recently in epitaxial thin films and even in nanowires, demonstrating the physical reality of the topological electromagnetic fields in solids [25].

A large number of Skyrmion based innovative devices have been recently proposed [26–28], although there remains several important issues to be resolved [22] before practical applications can be made. A notable Skyrmion based memory device is the Skyrmion racetrack memory, which has received considerable attention [26]. While a prototype racetrack memory has been success-fully demonstrated, a practical electrical read-out scheme still remains to be developed. Another intriguing idea is the use of a single Skyrmion as the information bit [29]. Research on the magnetic Skyrmions is currently in its infancy, with rapid development in the fundamental physics and applications expected in the coming years.

8. ACKNOWLEDGMENTS

References

[1] Skyrme, T. H. R. 1962, "A unified field theory of mesons and baryons", Nucl. Phys. **31**, 556-569

[2] Bogdanov, A. N. and Yablonskii, D. A. 1989, "Thermodynamically stable vortices in magnetically ordered crystals: The mixed state of magnets", Soviet Phys. JETP **68**, 101-103

[3] For a review, see: Salomaa, M. and Volovik, G. E. 1987, "Quantized vortices in superfluid ^{3}He", Rev. Mod. Phys. **59**, 533-613

[4] For a review of recent works, see: Nagaosa, N. and Tokura, Y. 2013, "Topological properties and dynamics of magnetic Skyrmions", Nature Nanotechnol. **8**, 899-911

[5] Mechelen, T. V. and Jacob, Z. 2019, "Viscous Maxwell-Chern-Simons theory for topological electromagnetic phases of matter", arXiv:1910.14288v1 (2019); Mechelen, T. V. and Jacob, Z. 2019, "Nonlocal topological electromagnetic phases of matter", Phys. Rev. B **99**, 205146.

[6] Garel, T. and Doniach, S. 1982, "Phase transitions with spontaneous modulation - the dipolar Ising ferromagnet," Phys. Rev. B **26**, 325-329

[7] Heinze, S. *et al.* 2011, "Spontaneous atomic-scale magnetic Skyrmion lattice in two dimensions," Nature Phys. **7**, 713-718

[8] Okubo, T., Chung, S. and Kawamura, H. 2012, "Multiple-q states and the Skyrmion lattice of the triangular-lattice heisenberg antiferromagnet under magnetic fields," Phys. Rev. Lett. **108**, 017206

[9] Brey, L. 2017," Magnetic Skyrmionic Polarons," Nano Lett. **17**, 7358-7363

[10] Mühlbauer, S., Binz, B. , Jonietz, F. , Pfleiderer, C. , Rosch, A., Neubauer, A., Georgii, R. and Boni, P. 2009, " Skyrmion lattice in a chiral magnet," Science **323**, 915

[11] Yu, X. Z. , Onose, Y., Kanazawa, N., Park, J. H., Han, J. H., Matsui, Y., Nagaosa, N. and Tokura, Y. 2010, "Real-space observation of a two-dimensional skyrmion crystal", Nature **465**, 901-904

[12] Shanavas, K. V. and Satpathy, S. 2016, "Electronic structure and the origin of the Dzyaloshinskii-Moriya interaction in MnSi," Phys. Rev. B **93**, 195101

[13] Yu, X. Z. , Kanazawa, N., Onose, Y., Kimoto, K., Zhang, W. Z., Ishiwata, S., Matsui, Y. and Tokura, Y. 2011, "Near room-temperature formation of a Skyrmion crystal in thin-films of the helimagnet FeGe," Nat. Mater. **10**, 106

[14] Ohuchi, Y. *et al.* 2018, "Electric-field control of anomalous and topological Hall effects in oxide bilayer thin films," Nat. Commun. **9**, 213

[15] Wang, L. *et al.* 2018, "Ferroelectrically tunable magnetic Skyrmions in ultrathin oxide heterostructures", Nat. Mater. **17**, 1087-1094

[16] Derrick, G. H. 1964, "Comments on Nonlinear Wave Equations as Models for Elementary Particles", J.Math. Phys., **5**, 1252

[17] Mohammad, M. V. and Satpathy, S. 2018, "Dzyaloshinskii-Moriya interaction in the presence of Rashba and Dresselhaus spin-orbit coupling", Phys. Rev. B, **97**, 094419

[18] Wilson, M. N. , Butenko, A. B., Bogdanov, A. N. and Monchesky, T. L. 2014, "Chiral Skyrmions in cubic helimagnet films: The role of uniaxial anisotropy", Phys. Rev. B, **89**, 094411

[19] Bruno, P., Dugaev, V. K. and Taillefumier, M. 2004, "Topological Hall effect and Berry phase in magnetic nanostructures", Phys. Rev. Lett., **93**, 096806

[20] The Feynman Lectures on Physics Vol III Ch. 21, "The Schrödinger Equation in a Classical Context: A Seminar on Superconductivity".

[21] Rashba, E. I. 1960, " Properties of semiconductors with an extremum loop. 1. Cyclotron and combinational resonance in a magnetic field perpendicular to the plane of the loop", Sov. Phys. Solid State **2**, 1109 ; Bychkov, Y. A. and Rashba, E. I. 1984, " Oscillatory effects and the magnetic susceptibility of carriers

in inversion layers", J. Phys. C **17**, 6039

[22] Finocchio, G., Büttner, F. , Tomasello, R., Carpentieri, M., Kläui, M. 2016 " Magnetic Skyrmions: from fundamental to applications", J Phys D Appl Phys, **49**, 423001

[23] Neubauer, A. *et al.* 2009, "Topological Hall effect in the A phase of MnSi", Phys. Rev. Lett. **102**, 186602

[24] Ranieri, E. D. 2014, "Skyrmions at the interface", Nature Nanotechnology **101**, 10.1038

[25] Schulz, T. *et al.* 2012, "topological electrodynamics of Skyrmions in a chiral magnet", Nature Phys. **8**, 301304

[26] Kang, W., Zheng, C., Huang, Y., Zhang, X., Zhou, Y., Lv, W., Zhao, W. 2016 "Complementary Skyrmion Racetrack Memory with Voltage Manipulation", IEEE Electron Device Letters, **37**, 924-927

[27] Liu, R.H., Lim, W.L. , Urazhdin, S. 2015 "Dynamical Skyrmion State in a Spin Current Nano-Oscillator with Perpendicular Magnetic Anisotropy", Phys. Rev. Lett. **114** , 137201

[28] Zhang, X. , Zhou, Y., Ezawa, M. , Zhao, G.P., Zhao, W. 2015 "Magnetic Skyrmion transistor: Skyrmion motion in a voltage-gated nanotrack", Sc. Rep. **5**, 11369
fundamental to applications", J Phys D Appl Phys, **49**, 423001

[29] Hagemeister, J., Romming, N., von Bergmann, K. , Vedmedenko, E.Y., Wiesendanger, R., 2015 " Stability of single Skyrmionic bits", Nat. Commun., **6**, 8455